

RSC Advances



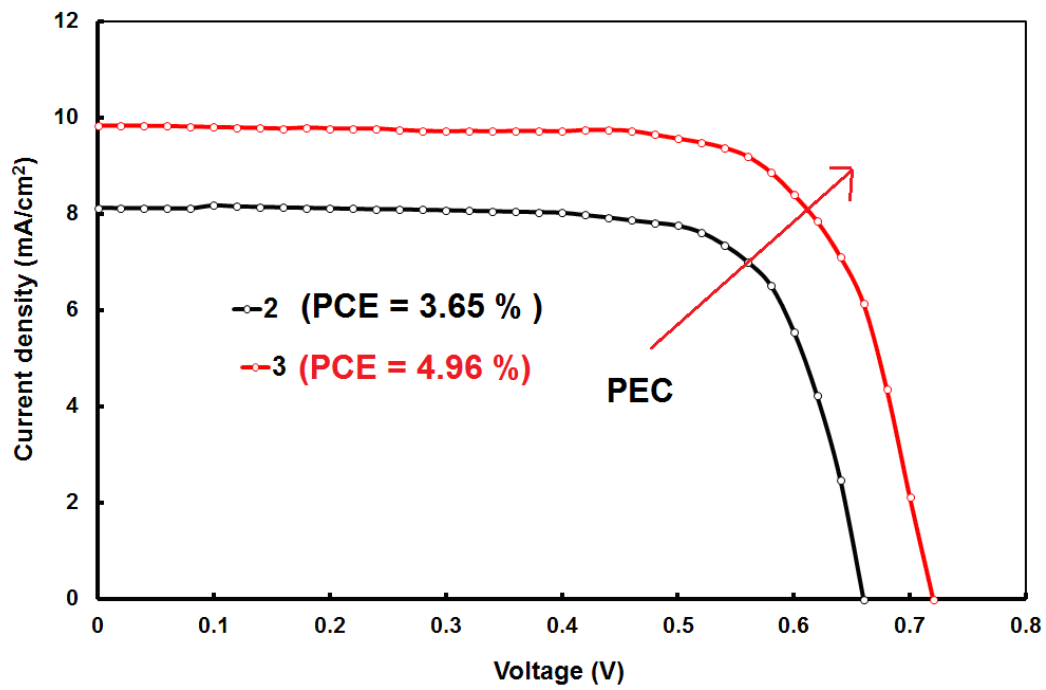
This is an *Accepted Manuscript*, which has been through the Royal Society of Chemistry peer review process and has been accepted for publication.

Accepted Manuscripts are published online shortly after acceptance, before technical editing, formatting and proof reading. Using this free service, authors can make their results available to the community, in citable form, before we publish the edited article. This *Accepted Manuscript* will be replaced by the edited, formatted and paginated article as soon as this is available.

You can find more information about *Accepted Manuscripts* in the [Information for Authors](#).

Please note that technical editing may introduce minor changes to the text and/or graphics, which may alter content. The journal's standard [Terms & Conditions](#) and the [Ethical guidelines](#) still apply. In no event shall the Royal Society of Chemistry be held responsible for any errors or omissions in this *Accepted Manuscript* or any consequences arising from the use of any information it contains.

Graphical abstract



Synthesis, optical and electrochemical properties of new ferrocenyl substituted triphenylamine based donor-acceptor dyes for dye sensitized solar cells

Rajneesh Misra^{*1}, Ramesh Maragani¹, K.R. Patel² and G. D. Sharma^{*3}

¹Department of Chemistry

Indian Institute of Technology, Indore (MP), India

Department of Physics

²Department of Physics, Jai Narayan Vyas University, Jodhpur (Raj.) 342005

³R & D Center for Engineering and Science

³JEC group of Colleges, Jaipur Engineering College, Kukas, Jaipur (Raj.) 302028, India

Abstract:

Two new ferrocenyl substituted triphenylamine based donor-acceptor dyes **D1** and **D2** were synthesized used as sensitizer for dye sensitized solar cells (DSSCs). The DSSC based on **D2** shows higher power conversion efficiency of 4.96% as compared to dye **D1** (PCE = 3.65%). The higher value of PCE was ascribed to the increase in the light harvesting property of the dye **D2** due to its extended absorption profile up to near infrared region and higher value of dye loading on the photoanode surface. The observed value of higher PCE has been also confirmed by the electrochemical impedance data and dark current.

Key words: Ferrocenyl substituted triphenylamine dyes, dye sensitized solar cells, power conversion efficiency,

*** corresponding authors**

E-mail : gdsharma273@gmail.com and sharmagd_in@yahoo.com (G.D.Sharma)
rajneeshmisra@iiti.ac.in (Rajneesh Mishra)

Introduction:

Dye sensitized solar cell (DSSCs), since the first reported by O'Regan and Grätzel in 1991^[1], have drawn considerable research interest as promising alternatives to conventional solar cells based on silicon, due to their low cost simplicity of fabrication and high overall power conversion efficiency (PCE) values.^[2] DSSCs typically consists of four components: a nanocrystalline wide energy bandgap metal oxide semiconductor film (generally TiO₂ or ZnO), a dye, an electrolyte or hole transport material, and a counter electrode. Upon light illumination, the light absorbed by sensitizer, excited electrons of the sensitizer are injected into the TiO₂ conduction band and transferred to the counter electrode through external load, and finally to I₃⁻, which yields I⁻ that reduces the photo-oxidized sensitizer to its original state. In above processes, the dye sensitizers play a vital role in both light harvesting and electron injection efficiency. In order to achieve an increased light harvesting efficiency in DSSCs, a variety of sensitizers were developed and tested. To date, DSSCs based on ruthenium based dyes^[3] and porphyrin dyes^[4] have shown very impressive PCEs. The DSSCs based on black dye with donor –acceptor type coadsorbent has reached an overall PCE of 11.4 %^[5], and a new record PCE of 12.3 %^[6] has been obtained by cosensitization of the porphyrin dye YD2-o-C8 and metal free organic dye. Although the sensitizers based on Ru complexes, showed high PCE but their low molar extinction coefficient, high cost as well as environmental concerns, limited their large scale applications. In this regards, metal free organic dyes have attracted great interest in recent years^[7] because of their unique advantages such as high absorption coefficient, ease of the structural modification, and relatively low cost and resulted their PCEs about more than 10 %^[8], rendering this type of molecules strong competitors to the ruthenium based sensitizers.

To develop high PCE DSSCs, many kinds of donor – π -acceptor (D- π -A) dyes possessing both electron donating (D) and electron withdrawing anchoring (A) groups linked by π -conjugated bridges, possessing broad and intense absorption features, have been developed so far, and would be especially expected to be one of the most class of metal free organic sensitizers [8a]. In D- π -A structure, triphenylamine derivatives have been widely used as the electron donor (D), whereas cyanoacrylic acid moiety as the electron acceptor as well as anchoring unit. Recently, ferrocene-based compounds, which exhibit chemical and electrochemical properties that are interesting for numerous applications, have been employed as donor units in sensitizers for DSSCs⁹. For example, Singh et al. have used some ferrocene based dithiocarbamate sensitizers for DSSCs.^[10,11] Recently, same research group

used ferrocenyl bearing Ni(II) and Cu(II) dithiocarbamates as sensitizers for DSSCs and achieved a PCE of 3.87%.^[12] However these dyes contain metal in the central position, which increases the complexity in their synthesis.

Herein, we have synthesized and investigated the optical and electrochemical properties of two ferrocenyl substituted triphenylamine (TPA) based donor-acceptor dyes **D1**, and **D2** for their application as sensitizers for DSSCs. The ferrocenyl is donor unit and can extend the absorption band towards the longer wavelength region whereas the cyanoacrylic acid acts as anchoring unit. The DSSC based on sensitizer **D2** showed higher PCE than that for sensitizer **D1**, attributed to the higher amount of dye loading and light harvesting efficiency.

Experimental details

The photoanodes of DSSCs were prepared on fluorine doped tin oxide (FTO) coated glass substrates, which were first cleaned by sonication subsequently with de-ionized water, iso-propanol and ethanol and then dried in air. The working electrodes were prepared by firstly forming a blocking layer of 0.2M titanium di-isopropoxide bis(acetylacetonate) in iso-propanol by spray pyrolysis on a pre-cleaned FTO coated glass substrate. This was followed by deposition of a nano-crystalline layer of TiO₂ by the doctor blade technique, using a dye sol TiO₂ paste (DSL 18NR-T). The TiO₂ coated FTO electrodes were heated at 500°C for 30 min. After cooling to room temperature, they were immersed into a 0.02 M TiCl₄ aqueous solution for 20 minutes, washed with distilled water and ethanol, and annealed again at 500°C for 20 min. The thickness of the TiO₂ layer was in the range of 10-12 μm. Finally, they were immersed into the corresponding solutions of **D1** and **D2** (5×10^{-4} M in dichloromethane) for 12 h and washed with dichloromethane to give the dye-sensitized TiO₂ working electrodes. The counter electrode was prepared by spin coating of a H₂PtCl₄(aq) solution (0.002 g of Pt in 1mL of iso-propanol) onto a pre-cleaned FTO coated glass substrate and then heating at 450° C for 15 min in air. The sensitized working electrode was assembled with the Pt coated FTO electrode into a sandwich type cell and sealed with the hot-melt polymer surlyn. To complete the DSSC fabrication, the electrolyte solution containing LiI (0.05M), I₂ (0.03 M), 1 methyl-3-n-propylimidazolium iodide (0.6M) and 0.5M *tert*-butylpyridine in a mixture of acetonitrile and valeronitrile (85:15 volume ratio) was introduced into the space between the two electrodes through a pre-drilled hole in the platinum coated FTO by vacuum backfilling.

The current-voltage (*J-V*) characteristics of the DSSCs under simulated air mass 1.5 global, and illumination intensity of 100mW/cm² were measured by a computer controlled

Keithley source meter and illuminated using the solar simulator. The incident photon to current efficiency (IPCE) of the devices was measured illuminating the device through the light source and monochromator and resulting current was measured using Keithley electrometer under short circuit condition.

Electrochemical impedance spectra (EIS) in dark were recorded using a CH electrochemical workstation. They were measured by applying a dc bias equivalent to the open circuit voltage of DSSC in the frequency range 0.1 to 100 KHz with ac signal of 20 mV.

Results and discussion

The intermediate 4-(Bis-(4-iodo-phenyl)-amino]-benzaldehyde was synthesized from 4-(diphenylamino)-benzaldehyde according to the literature reported procedure.^[13] The compound **1** was synthesized by the Sonogashira cross-coupling reaction of the 4-(Bis-(4-iodo-phenyl)-amino]-benzaldehyde with ethynyl ferrocene (See ESI for details).^[14] The Knoevenagel condensation reaction of **1** with cyanoacetic acid in dichloromethane, and acetic acid mixture (1:1) as a solvent in the presence of NH₄OAc resulted compound **D2** in 81% yield. The [2 + 2] cyclo-addition reaction of donor-acceptor compound **D2** with tetracyanoethylene (TCNE) at 75 °C, in dichloromethane solvent in microwave resulted compound **D3** in 60% yield (Scheme 1).

Photophysical properties

The electronic absorption spectra of the ferrocenyl substituted triphenylamine based donor-acceptor **D1** and **D2** dyes in dilute dichloromethane solution are shown in Figure 1 and the data are listed in Table 1. The UV-vis absorption spectrum of the dye **D1** shows two types of bands. The first band in the region 353 nm and near 300 nm for **D1** and **D2** corresponding to $\pi \rightarrow \pi^*$ transition, and the second band in the region 450-470 nm corresponding to intramolecular charge transfer (ICT).^[15]

The dye **D2** shows, the first high energy absorption band around 471 nm corresponding to $\pi \rightarrow \pi^*$ transition, and the second low energy broad band around 630-700 nm corresponding to ICT (Figure 1).^[16]

The absorption spectra of **D1** and **D2** on TiO₂ film are shown in Figure 2. The maximum absorption peaks for **D1** and **D2** on to TiO₂ films are about 474 nm and 492 nm, respectively. The absorption band of **D1** and **D2** dyes on TiO₂ films are red shifted by 18 nm and 11 nm, respectively as compared in solution. This red shift can be explained by the formation of J aggregation or electronic coupling of the dye on TiO₂ surface.^[17] It was reported that smaller shift in λ_{\max} associated with dyes from solution vs thin film suggest a

smaller tendency to form dye aggregates on the semiconductor surface. This phenomena result to higher photocurrent densities.^[18] It should be noted here that the redshift for the dye **D2** is less than that for dye **D1**, indicating that the incorporation of TCNE acceptor group could suppress the formation of aggregates effectively on the TiO₂ surface. Furthermore, the absorption band of dye **D2** on the TiO₂ surface became broader compared to that of dye **D1**, since the former one might originate from the electronic transition bands of TPA. Therefore, the strong light harvesting ability of dye **D2** with less aggregation on TiO₂ film would be favorable the performance of DSSCs.^[19] The optical band gap was estimated from the onset of the absorption of absorption spectra of dye adsorbed onto TiO₂ film, and is 2.17 eV and 1.74 eV for **D1** and **D2**, respectively.

To obtain information about the binding of these dyes onto the TiO₂ surface of the electrode of the DSSC, the Fourier transform infrared (FTIR) spectra of pristine dye powder and that of dyes adsorbed on TiO₂ were measured. The FTIR spectra of dye **D1** and **D2** showed absorption band around 1694 cm⁻¹, assigned to the free carboxylic acid groups of the powdered **D1** and **D2** dyes. However, FTIR spectra of dye sensitized TiO₂ films displayed two characteristic bands at 1586 cm⁻¹ and 1348 cm⁻¹, assigned to the COO⁻ anti-symmetric and symmetric stretching vibrations of carboxylate groups, respectively, coordinated with surface titanium atoms and the band around 1694 cm⁻¹ completely disappeared. These observations suggested that there is a strong binding and electronic coupling of these dyes through the carboxylic acid group onto the TiO₂ surface.^[20]

Electrochemical properties

The electrochemical properties of the ferrocenyl substituted triphenylamine based donor-acceptor **D1** and **D2** dyes were studied by the cyclic voltammetry (CV) analysis. The CV data has been reported here with respect to Ferrocene oxidation (Fc/Fc⁺ = 0.00 V). Cyclic voltammograms of these dyes are shown in Figure 3 and corresponding data are summarized in table 2. The cyclic voltammogram of compound **D1** show two oxidation waves; (a) the reversible wave in the region 0.08 V corresponding to the oxidation of ferrocene unit, (b) the quasi reversible oxidation wave in the region 0.65 V, which belongs to the triphenylamine unit.^[21]

The cyclic voltammogram of donor-acceptor compound **D2** show two oxidation waves, and two reduction waves. The first oxidation wave in the region 0.39 V corresponding to the oxidation of ferrocene unit, and the second quasi reversible wave in the region 1.02 V which belongs to triphenylamine unit. The two reduction waves, one is quasi reversible in the

region of 0.97 V, and another one is reversible in the region of 1.39 V belongs to the TCNE group.^[22] The **D2** exhibit higher oxidation potential compared to **D1** and attributed to the increase in the number of acceptors i.e. TCNE acceptors units.

As shown in Table 1, the oxidation potential (E_{ox}) due to the triphenylamine unit, (0.65 V for dye **D1** and 1.02 V for dye **D2** with respect to $Fc/Fc^+ = 0.00$ V) has been considered for the HOMO level. These values are converted with respect to NHE and are 0.52 V and 0.83 V vs NHE, which are more positive than I_3^-/I^- redox couple (0.4 V vs NHE), indicating that the oxidized dyes formed after electron injection into the conduction band of TiO_2 could be thermodynamically accept electrons from I^- ions. In particular, the lower value of HOMO observed for dye **D2** implies that DSSC made with it may show the higher efficient charge regeneration.^[23] The LUMO levels of the sensitizers were estimated by the values of E_{ox} and the optical band gaps i.e. $E_{LUMO} = -(E_{opt} - E_{HOMO})^{17a}$ and the latter values were calculated by the onset of absorption spectra in Figure 2. The LUMO values of dye **D1** (-1.65 V vs NHE) and **D2** (-0.91V vs NHE) are more negative than the conduction band edge of TiO_2 (-0.5 V vs NHE), indicating the electron injection from LUMO of these sensitizers to conduction band is energetically feasible. The reduction potential of the **D2** was observed about -1.39 V vs Fc^+/Fc which is different from that estimated from the difference in E_{opt} and E_{HOMO} , may be attributed to reorganization energy needed to optically excited the molecule is not the same as reducing it. Therefore, these dyes could be used as sensitizers for DSSCs.

Theoretical calculations

Density functional theory (DFT) is a popular method for ground state electronic structure calculations. In case of donor acceptor systems DFT calculation are extensively performed to explore their donor-acceptor character along with determination of the HOMO and LUMO energy level. DFT calculations of ground state energies, structures, and many other properties are routinely performed. However, because photoexcited molecules are experimentally much more difficult to characterize than molecules in their ground states time-dependent density functional theory (TDDFT), method is used to treat excited states in a DFT framework. DFT calculation is reliable method for determining ground state energies and structures for various types of donor-acceptor systems. Thus, to get an elementary idea about the electronic structure and determination of HOMO and LUMO energy level of the dye **D1** and **D2** we performed the DFT calculation with Gaussian 09 at the B3LYP/6-31G**

for C, H, N, O, and Lan12DZ for Fe level.^{24,25} We have explored similar type of ferrocene based systems utilizing the DFT method and got satisfactory results.^{22c} The ferrocenyl groups were found to be almost planar with respected to the phenyl ring in **D1** dye. On the other hand the incorporation of the TCNE group results in loss of planarity of ferrocenyl groups due to steric hindrance in **D2**. The optimized structures of **D1**, and **D2** are shown in Figure 4.

The Mulliken spin density distribution of **D1** and **D2** are shown in Figure 5. The both **D1** and **D2** show high electron density on the nitrogen (-0.570) and oxygen atoms (-0.567), whereas the neighbor carbon atoms show less electron density (0.570). The spin densities on the ferrocenyl groups are practically zero in all the cases (Figure 5).

In **D1** dye the HOMO orbitals are localized on the both ferrocene and the triphenylamine units, whereas the LUMO orbitals are mainly concentrated on the acceptor unit (cyanoacetic acid). The contribution of the HOMO and LUMO orbitals in **D2** dye undergoes a drastic change, due to the incorporation of the 1,1, 4,4-tetracyanobuta-1,3-diene (TCBD) unit. Careful analysis of the frontier molecular orbitals reveals that main transition takes place from HOMO-1 to LUMO+1 in **D2**. The HOMO-1 and LUMO+1 molecular orbital indicate that electron density is occupied on one of the TCNE unit as well as cyanoacetic acid group (anchor moiety). So this electronic structure full fills the requirement for electron injection from the LUMO level of **D2** into the conduction band of TiO₂ electrode.

Photovoltaic properties

The photovoltaic properties of the fabricated DSSCs sensitized **D1** and **D2** dyes under stimulated light irradiation (100 mW/cm²) are shown in Figure 7a. The detailed photovoltaic parameters such as short circuit photocurrent (J_{sc}), open circuit voltage (V_{oc}), fill factor (FF) and power conversion efficiency are compiled in Table 2. The PCE of the DSSC sensitized with dye **D1** and dye **D2** are about 3.65 % and 4.96 %, respectively. The higher value of PCE for DSSCs sensitized with **D2** illustrated that the introduction of TCNE acceptor in the conjugated arms improves the PCE of the DSSC. The values of J_{sc} , V_{oc} and FF for the DSSC sensitized with **D2** are higher than that for **D1**. The increased value of J_{sc} attributed to broader absorption profile of dye **D2** adsorbed on TiO₂ and higher amount of dye loading whereas the increase in the V_{oc} could be attributed to the effective retardation of charge recombination between the injected electrons in the TiO₂ and oxidized dye **D2**.^[26] The origin of the increased value of V_{oc} can also be justified from the J-V characteristics of the DSSCs in dark as shown in Figure 7b. It can be seen from Figure 7b that the onset of the dark current for

DSSC sensitized with **D2** is higher than that for **D1**, indicating that the increase in V_{oc} was associated with decreasing of the electron recombination in TiO_2 with the I_3^-/I^- redox couple in the electrolyte.^[27] The lower value of V_{oc} for the DSSC sensitized with dye **D1** than that of dye **D2** may be due to higher level of ground state oxidation potential of **D1** (0.52 V vs NHE) than **D3** (0.83 V vs NHE), which enhanced the back electron transfer from the conduction band to the oxidized dye.

The incident photons to current efficiency (IPCE) spectra of the DSSCs are shown in Figure 8. The IPCE spectra of these devices closely resembles with the absorption spectra of the respective dyes adsorbed onto the TiO_2 surface. The IPCE spectra of DSSC based on **D2** extends to the longer wavelength region as compared to **D1**. This feature is in agreement with the trend in absorption spectra. The IPCE of the DSSC can be expressed as

$$IPCE = LHE \times \eta_{inj} \times \eta_{cc}$$

Where LHE is the light harvesting efficiency (which depends upon the absorption profile and amount of dye adsorbed on the TiO_2 surface), η_{inj} is the electron injection efficiency (depends upon the electron injection rate from the sensitizer into the conduction band of TiO_2), and η_{cc} is the charge collection efficiency (depends upon the electron transport rate in TiO_2 towards the FTO electrode and the recombination of the electrons with the redox couple in the electrolyte and oxidized dye).

Another critical factor in determining the PCE and IPCE values of DSSCs is the LHE of the photoanode.^[28] The IPCE values for the DSSC sensitized with dye **D2** are higher than that for **D1** at all wavelengths. As can be seen from the Figure 2 that the absorption profile of **D2** is more extended to higher wavelength region as compared to **D1**, the higher values of IPCE may attributed to enhanced light LHE for DSSC based sensitized with **D2**. This shows that enhanced LHE can increase the photocurrent and IPCE values.

In general, the V_{oc} is determined by difference between the quasi Fermi level of electron in dye sensitized TiO_2 electrode under illumination and the redox potential level of the redox couple in the electrolyte. Since the electrolyte used in both DSSCs is same, the value of the V_{oc} depends upon the Fermi level for electrons after the electron injection in both dyes. The V_{oc} value of the DSSCs can be expressed as^[7c]

$$V_{oc} = \left(\frac{E_{CB}}{q} \right) + \left(\frac{kT}{q} \right) \ln \left(\frac{n_c}{N_{CB}} \right) - \left(\frac{E_{red}}{q} \right)$$

Where E_{CB} is the TiO_2 conduction band edge, E_{red} is the electrolyte redox potential, kT represents the thermal energy, n_c and N_{CB} are the number of electrons and density of states in TiO_2 conduction band, respectively. After the dye sensitization on the TiO_2 surface, a shift of ΔE_{CB} takes place and can be given by the expression:^[29]

$$\Delta E_{CB} = \frac{-q\mu_{normal}\gamma}{\epsilon_0\epsilon}$$

Where μ_{normal} is the dipole moment of the absorbed dye vertically to the TiO_2 surface, γ is the concentration of dye molecules adsorbed on the TiO_2 surface (dye loading) ϵ_0 and ϵ are the permittivity of vacuum and dielectric constant of dye monolayer, respectively. From above expression, it is apparent a dye with larger μ_{normal} and γ yield a larger shift in the conduction band edge, leading to the higher value of V_{oc} . Since the dipole moment of **D2** is larger than that of **D1** and dye loading is higher for DSSC based on **D2** sensitized photoanode than **D1**, therefore, the ΔE_{CB} is larger for DSSC based on dye **D2** and consequently the DSSC based on **D2** results higher value of V_{oc} .

To further investigate the photovoltaic properties of DSSCs sensitized with these two dyes, electrochemical impedance spectroscopy (EIS) was performed.^[30,31] The EIS analysis of DSSCs were recorded in the dark under a forward bias voltage of -0.68 V, i.e. equivalent to the approximately V_{oc} of the DSSC and in the frequency range from 0.1 Hz to 100 KHz. The Nyquist plots of the EIS of the DSSCs based on **D1** and **D2** are shown in Figure 8a. Generally in the Nyquist plot of EIS spectra three semicircles were observed. The smaller semicircle at high frequency is assigned to the redox charge transfer response at the counter electrode/electrolyte interface.^[31] The large one at the intermediate frequency represents the electron transfer process at the TiO_2 /dye/electrolyte interface. In the low frequency region, the impedance is associated with the Warburg diffusion process of I_3^- / I^- in electrolyte. The two DSSCs showed minimal differences in the smaller semicircles observed at higher frequencies due to the same Pt and electrolyte, however, the difference in between the DSSCs in the intermediate frequency semicircle was significant. The charge recombination resistance (R_{rec}) at the TiO_2 /dye /electrolyte interface can be estimated by fitting the semicircle in the intermediate frequency region using Z-view software. This resistance is related to the charge recombination rate, i.e. smaller R_{rec} indicates a faster charge recombination and therefore a larger dark current. It can be seen from the figure that the radius of the semicircle in intermediate region is lower for the DSSC sensitized with **D2** as compared to that for **D1**.

This is consistent with the higher value of V_{oc} for the DSSC based on **D2** as compared to that for **D1**.

The electron lifetime was estimated from the peak frequency (f_{peak}) at the frequency region corresponds to the TiO_2 /dye/electrolyte interface in Bode phase plot (Figure 8b), according the $\tau_e = 1/2\pi f_{peak}$. The estimated value of electron lifetimes for the DSSC based on **D1** and **D2** are 17.80 ms and 23.46 ms, respectively, indicating the back charge recombination is suppressed for the DSSC sensitized with **D2** as compared to **D1**.

Conclusion

In summary, we have designed and synthesized donor-acceptor type ferrocenyl substituted triphenylamine based **D1** and **D2** dyes and applied as sensitizers for DSSCs. The effect of TCNE acceptor group on the optical, electrochemical and photovoltaic properties was investigated. The DSSC based on dye **D2** yielded a PCE of 4.96 % ($J_{sc} = 9.84 \text{ mA/cm}^2$, $V_{oc}=0.72$ and $FF = 0.70$) while dye **D1** showed a PCE of 3.65% ($J_{sc}=8.13 \text{ mA/cm}^2$, $V_{oc} = 0.66 \text{ V}$ and $FF= 0.68$). The J_{sc} of dye **D2** is higher than dye **D1** which can be attributed to the broader absorption profile of dye **D2** and higher value of IPCE. At the same time the EIS results are in good agreement with the different V_{oc} values for DSSCs based on two dyes. The higher value of V_{oc} can be further explained by the longer electron lifetime. These dyes are easily to synthesis as compared to other metal free dyes and therefore the cost can be further lowered using this type of metal free dyes.

References

1. B. O. Regan, and M. Grätzel, *Nature*, 1991, **353**, 737-740.
2. (a) S. Zhang, X. Yang, Y. Numata and L. Han, *Energy Environ. Sci.*, 2013, **6**, 1443; (b) J. Gong, J. Liang, and K. Sumathy, *Renewable and Sustainable Energy Reviews*, 2012, **16**, 5848–5860; (c) Z. S. Wang, H. Kawauchi, T. Kashima, and H. Arakawa *Coordination Chemistry Reviews*, 2004, **248**, 1381–1389.
3. K. L. Wu, C. H. Li, Y. Chi, J. N Clifford, L. Cabau, E. Palomares, Y. M. Cheng, H. A. Pan and P. T. Chou, *J. Am. Chem. Soc.* 2012, **134**, 7488–7496.
4. (a) B. Liu, W. Zhu, Y. Wang, W. Wu, X. Li, B. Chen, Y. T. Long and Y. Xie, *J. Mater. Chem.* 2012, **22**, 7434; (b) H. Hayashi, A. S. Touchy, Y. Kinjo, K. Kurotobi, Y. Toude, S. Ito, H. Saarenp, N. V. Tkachenko, H. Lemmetyinen, and H. Imahori, *Chem. Sus. Chem.* 2013, **6**, 508-517; (c) B. R. Ambre, G. F. Chang, R. Manoj, B. Zanwar, C. F. Yao, E. W. G. Diau, and C. H. Hung, *Chem. Asian J.*, 2013, **8**, 2144 –

- 2153, (d) T. Bessho, S. M. Zakeeruddin, C. Y. Yeh, E. W. G. Diau and M. Grätzel, *Angew. Chem. Int. Ed.* 2010 **49**, 6646–6649; (e) A. Yella, H. W. Lee, H. N. Tsao, C. Yi, A. K. Chandiran, M. K. Nazeeruddin, E. W. G. Diau, C. Y. Yeh, S. M. Zakeeruddin and M. Grätzel, *Science* 2011, **334**, 629; (f) L. L. Li and E. W. G. Diau, *Chem. Soc. Rev.* 2013, **42**, 291-304
5. L. Han, A. Islam, C. H. Malapaka, B. Chiranjeevi and S. Zhang, *Energy Environ. Sci.* 2012, **5**, 6057-6060.
6. A. Yella, H. W. Lee, H. N. Tsao, C. Y. Yi, A. K. Chandiran and M. K. Nazeeruddin, *Science*, 2011, **334**, 629-634
7. (a) B. G. Kim, K. Chung and J. Kim, *Chem. Euro.* 2013, **19**, 5220-5230; (b) R. K. Kanaparthi, J. Kandhadi and L. Giribabu, *Tetrahedron*, **2012**, 68, 8383-8393; (c) A. Mishra, M. K. R. Fischer and P. Buerle, *Angew. Chem. Int. Ed.* 2009, **48**, 2474–2499; (d) C. Qin, W. Y. Wong and L. Han, *Chem. Asian J.* 2013, **8**, 1706-1719; (e) M. Liang and J. Chen, *Chem. Soc. Rev.* 2013, **42**, 3453-3488, (f) S. Ahmad, E. Guillen, L. Kavan, M. Grätzel and M. K. Nazeeruddin, *Energy Environ. Sci.* 2013, **6**, 3439-3466 (g) Y. Wu and W. Zhu, *Chem. Soc. Rev.* 2013, **42**, 2039-2058
8. (a) W. Zeng, Y. Cao, Y. Bai, Y. Wang, Y. Shi, M. Zhang, F. Wang, C. Pan, and P. Wang, *Chem. Mater.* 2010, **22**, 1915; (b) M. Xu, S. Wenger, H. Bala, D. Shi, R. Li, Y. Zhou, S. M. Zakeeruddin, M. Grätzel and P. Wang, *J. Phys. Chem. C.* 2009, **113**, 296; (c) B. G. Kim, C. G. Zhen, E. J. Jeong, J. Kieffer and J. Kim, *Adv. Funct. Mater.* 2012, **22**, 1606; (d) S. Hwang, J. H. Lee, C. Park, H. Lee, C. Kim, C. Park, M.-H. Lee, W. Lee, J. Park, K. Kim, N.-G. Park and C. Kim, *Chem. Commun.* 2007, 4887.
9. (a) A. Togni and T. Hayashi, *Ferrocenes: Homogeneous Catalysis, Organic Synthesis, Material Science, VCH, Weinheim*, 1995; (b) E. M. Barranco, O. Crespo, M. C. Gimeno, P. G. Jones, A. Laguna and C. Sarroca, *Dalton Trans.*, 2001, 2523–2529
10. V. Singh, R. Chauhan, A. Kumar, L. Bahadur and N. Singh, *Dalton Trans.*, 2010, **39**, 9779
11. A. Kumar, R. Chauhan, K. C. Molloy, G. K. Köhn, L. Bahadur and N. Singh, *Chem.–Eur. J.*, 2010, **16**, 4307.
12. V. Singh, R. Chauhan, A. N. Gupta, V. Kumar, M. G. B. Drew, L. Bahadur and N. Singh, *Dalton Trans.* 2014, **43**, 4752-4761

13. (a) B. Xu, H. Fang, F. Chen, H. Lu, J. He, Y. Li, Q. Chen, H. Sun, and W. Tian, *New J. Chem.* 2009, **33**, 2457–2464; b) M. J. Lee, K. D. Seo, H. M. Song, M. S. Kang, Y. K. Eom, H. S. Kang and H. K. Kim, *Tetrahedron Lett.* 2011, **52**, 3879–3882.
14. R. Maragani, and R. Misra, *Tetrahedron*, 2014, **70**, 3390-3399
15. P. Leriche, P. Frere, A. Cravino, O. Aleveque and J. Roncali, *J. Org. Chem.* 2007, **72**, 8332- 8336.
16. (a) V. Nemykin, A. Y. Maximov and A. Y. Kuposov, *Organometallics* 2007, **26**, 3138-3148; b) X. Tang, W. Liu, J. Wu, C. S. Lee, J. You and P. Wang, *J. Org. Chem.* 2010, **75**, 7273–7278; c) B. Breiten, M. Jordan, D. Taura, M. Zalibera, M. Griesser, D. Confortin, C. Boudon, J. P. Gisselbrecht, W. B. Schweizer, G. Gescheidt and F. Diederich, *J. Org. Chem.* 2013, **78**, 1760–1767.
17. (a) X. Ren, Q. Feng, G. Zhou, C.-H. Huang, and Z. S. Wang, *J. Phys. Chem. C.*, 2010, **114**, 7190; (b) J. Tang, J. L. Hua, W. J. Wu, J. Li, Z. G. Jin, Y. T. Long and H. Tian, *Energy Environ. Sci.* 2010, **3**, 1736.
18. (a) S. Roquet, A. Cravino, P. Leriche, O. Alêvêque, P. Frère and J. Roncali, *J. Am. Chem. Soc.*, 2006, **128**, 3459.
19. C. Teng, X. Yang, C. Yang, H. Tian, S. Li, X. Wang, A. Hagfeldt, and L. Sun, *J. Phys. Chem. C.*, 2010 **114**, 11305.
20. (a) R. Grisorio, L. D. Marco, G. Allegretta, R. Giannuzzi, G. P. Suranna, M. Manca, P. Mastroilli, and G. Gigli, *Dyes Pigm.* 2013, **98**, 221; (b) D. Wang, R. Mendelsohn, E. Gopoppini, P.G. Hoertz, R.A. Carlisle, G. Meyer, *J. Phys. Chem. B.*, 2004, **108**, 16642; (c) G. E. Zervaki, E. Papastamatakis, P. A. Angaridis, V. Nikolaou, M. Singh, R. Kurchania, T. N. Kitsopoulos, G. D. Sharma, and A. G. Coutsolelos, *Eur. J. Inorg. Chem.* 2014, 1020-1033
21. (a) C. Teng, X. Yang, C. Yang, S. Li, M. Cheng, A. Hagfeldt and L. Sun, *J. Phys. Chem. C.*, 2010, **114**, 9101–9110; b) C. Sakong, H. J. Kim, S. H. Kim, J. W. Namgoong, J. H. Park, J. H. Ryu, B. Kim, M. J. Kob and J. P. Kim, *New J. Chem.*, 2012, **36**, 2025–2032.
22. (a) T. Mochida and S. Yamazaki, *J. Chem. Soc. Dalton Trans.* 2002, 3559–3564; b) T. Michinobu, H. Kumazawa, K. Noguchi and K. Shigehara, *Macromolecules* 2009, **42**, 5903– 5905. (c) R. Maragani, and R. Misra, *Tetrahedron*, 2014, **70**, 3390-3399.
23. Y. J. Chang, P. T. Chou, S. Y. Lin, M. Watanabe, Z. Q. Liu, J. L. Lin, K. Y. Chen, S. S. Sun, C. Y. Liu and T. J. Chow, *Chem.–Asian J.*, 2012, **7**, 572.

24. (a) A. D. Becke, *J. Chem. Phys.* 1993, **98**, 5648-5652; b) C. T. Lee, W. T. Yang and R. G. Parr, *Phys. Rev. B.* 1988, **37**, 785-789; c) P. J. Hay, W. R. Wadt, *J. Chem. Phys.* 1985, **82**, 270-283.
25. (a) M. M Francl, W. J. Pietro, W. J. Hehre, J. S. Binkley, M. S. Gordon, D. J. Defrees, and J. Pople, *J. Chem. Phys.* 1982, **77**, 3654-3665; b) F. Ding, S. Chen, and H. Wang, *Materials* 2010, **3**, 2668-2683.
26. (a) S. Y. Huang, G. Schlichthorl, A. J. Nozik, M. Gratzel, and A. J. Frank, *J. Phys. Chem. B.*, 1997, **101**, 2576; (b) T. Marinado, K. Nonomura, J. Nissfolk, M. K. Karlsson, D. P. Hagberg, L. Sun, S. Mori and A. Hagfeldt, *Langmuir*, 2010, **26**, 2592.
27. M. Liang, W. Xu, F. S. Cai, P. Q. Chen and B. Peng, J. Chen, Z. M. Li, *J. Phys. Chem. C*, 2007, **111**, 4465.
28. (a) H. Hayashi, K. Hosomizu and Y. Mantano, *J. Phys. Chem. B.* 2004, **108**, 5018; (b) S. Hayashi, S. Eu and H. Imahori, *Chem. Commun.* 2007, 2069.
29. (a) S.R^uhle, M. Greenshtein, S.-G. Chen, A. Merson, H. Pizem, C. S. Sukenik, D. Cahen and A. Zaban, *J. Phys. Chem. B.*, 2005, **109**, 18907, (b) W. L. Ding, D. M. Wang, Z. Y. Geng, X. L. Zhao and W. B. Xu, *Dyes Pigm.*, 2013, **98**, 125
30. (a) Q. Wang, J. E. Moser and M. Grätzel, *J. Phys. Chem. B.*, 2005, **109**, 14945-14953, (b) R. Kern, R. Sastrawan, L. Ferber, R. Stangl and J. Luther, *Electrochim. Acta.* 2002, **47**, 4213-4225.
31. M. Adachi, M. Sakamoto, J. Jiu, Y. Ogata and S. Isoda, *J. Phys. Chem. C* 2006, **110**, 13872

Table 1

Photophysical and electrochemical data of donor-acceptor **D1** and **D2** dyes

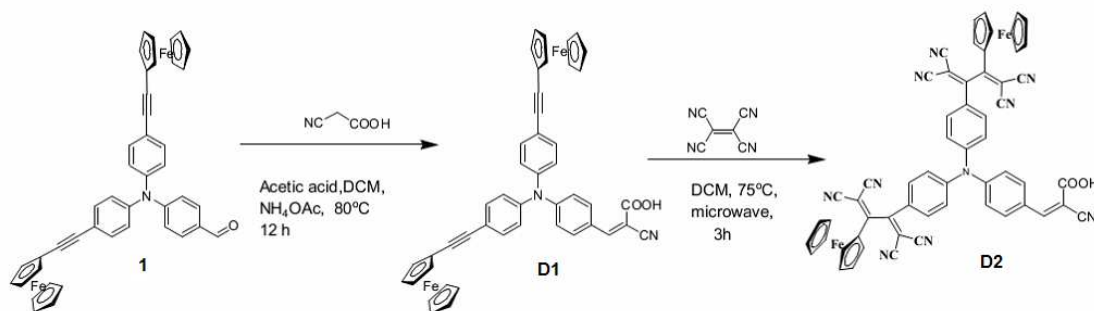
Compound	λ_{\max} (nm)	ϵ ($M^{-1} \text{ cm}^{-1}$) ^e	E_{oxid} (V)	E_{red} (V)	Optical band gap(eV) _f	Theoretical band gap (eV) ^g	Dipole moment (Debye) ^g
D1	353 450	28600	0.08 ^a 0.65 ^b	-	2.17	2.79	9.6031
D2	471 -	17045	0.39 ^a 1.02 ^b	-1.39 ^d -0.97 ^c	1.74	2.75	14.5274
Ferrocene	-	-	0.00	-	-	-	-

^a The oxidation value of ferrocenyl unit, and ^b the oxidation value of triphenylamine unit. ^{c,d} The reduction values of TCNE group. ^e Measured in dichloromethane solvent. ^f Optical band gap estimated from the absorption edge of absorption spectra of dye adsorbed onto TiO₂ film. ^g Theoretical values at B3LYP/6-31G** level.

Table 2

Photovoltaic parameters of DSSCs sensitized with dye **D1** and **D2**

Dye	J_{sc} (mA/cm ²)	V_{oc} (V)	FF	PCE (%)
D1	8.13	0.66	0.68	3.65
D2	9.84	0.72	0.70	4.96



Scheme 1. Synthesis of dye **D1** and **D2**

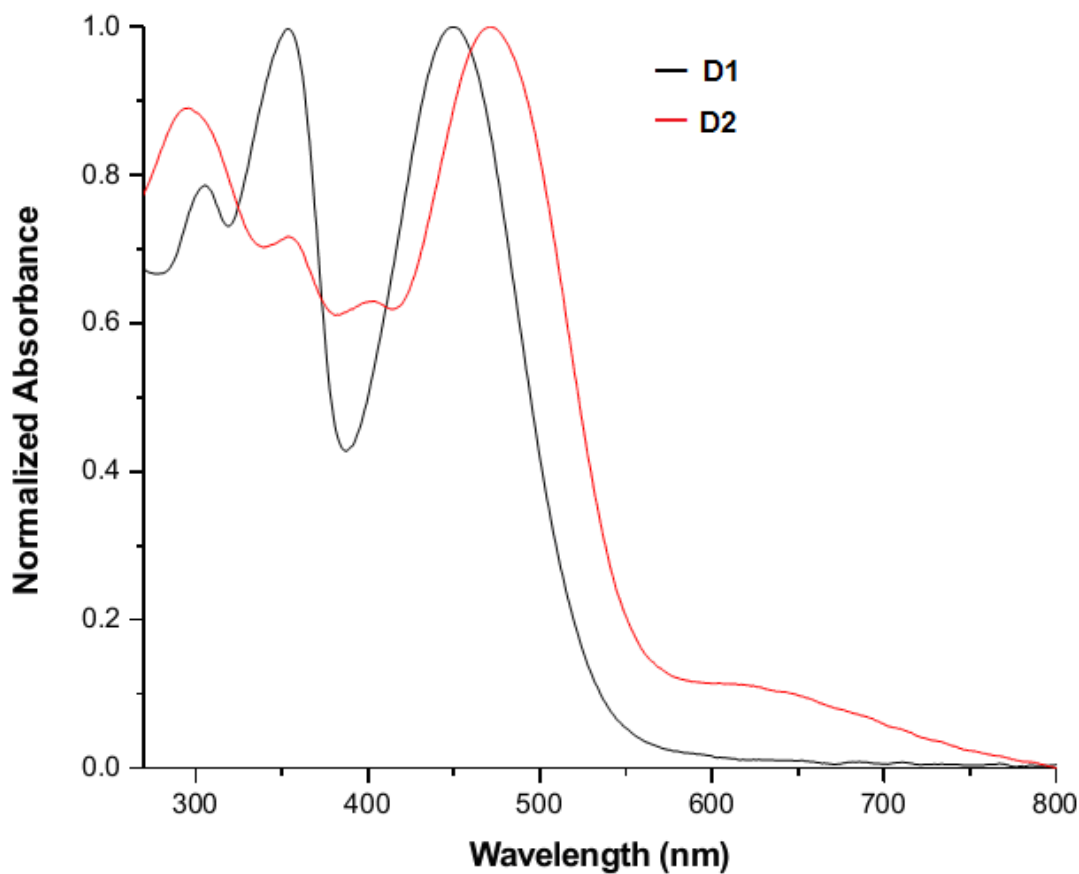


Figure 1. Normalized electronic absorption spectra of the ferrocenyl substituted triphenylamine based donor-acceptor compound **D1** and **D2** in CH₂Cl₂ (1.0 × 10⁻⁴ M).

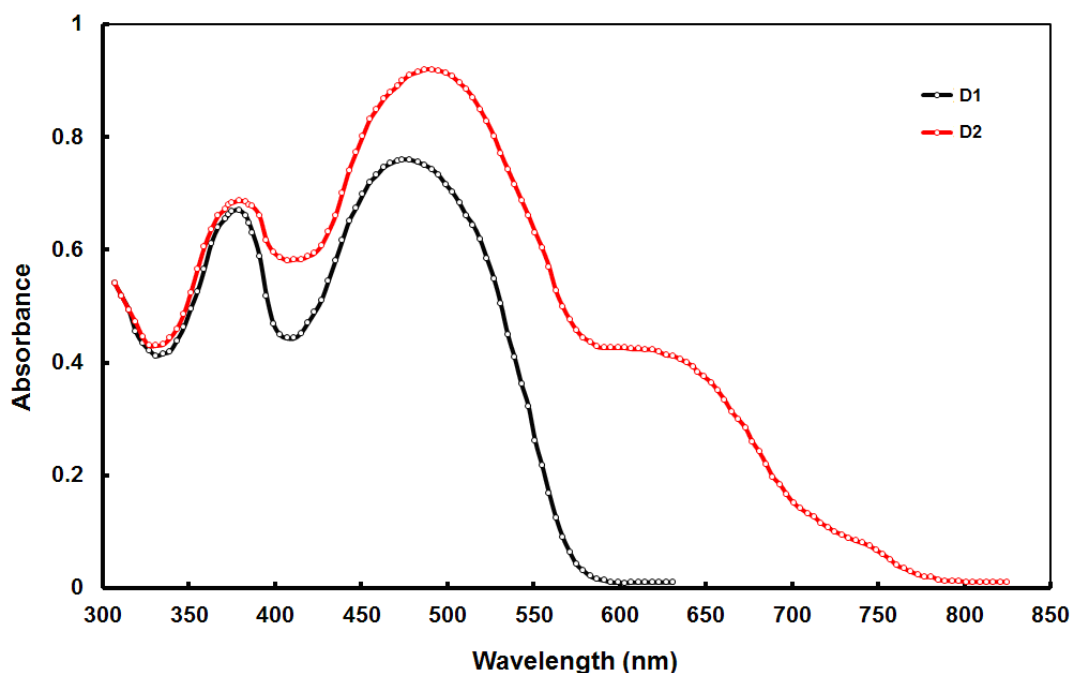


Figure 2. Normalized electronic absorption spectra of the ferrocenyl substituted triphenylamine based donor-acceptor **D1** and **D2** dyes adsorbed on TiO₂ film

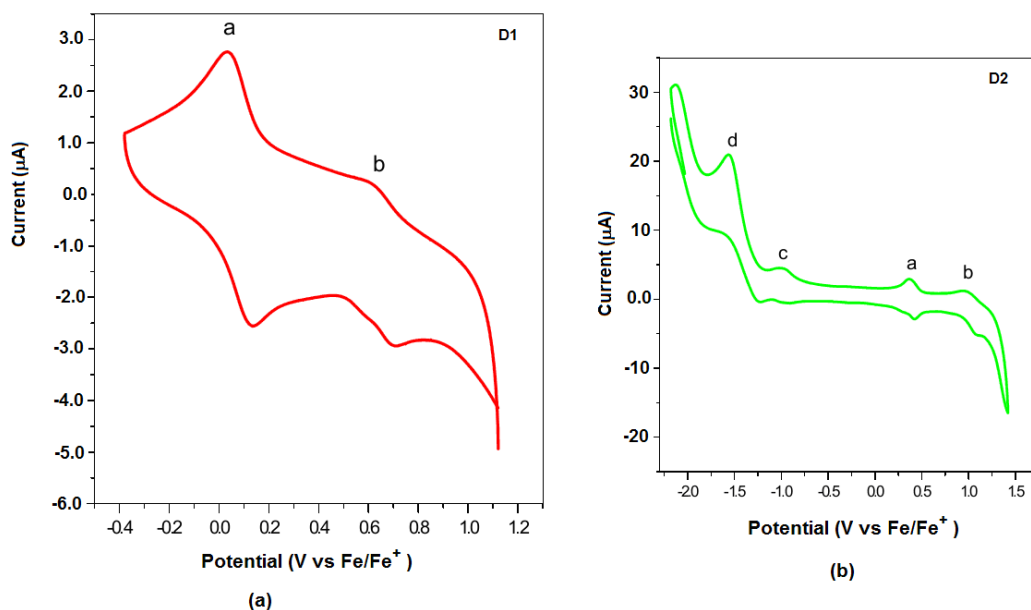


Figure 3. Cyclic voltammograms of the ferrocenyl substituted triphenylamine based donor-acceptor (a) dye **D1**, and (b) dye **D2**, at 1.0×10^{-4} M concentration in 0.1M TBAPF₆ in dichloromethane recorded at a scan rate of 100 mV s^{-1} .

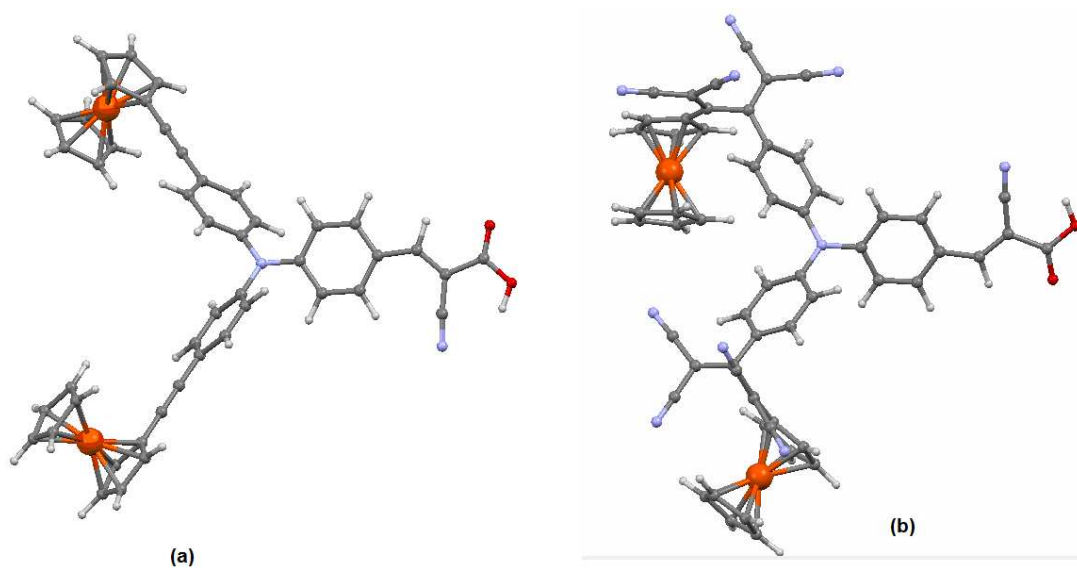


Figure 4. Geometry optimized structures of the ferrocenyl substituted triphenylamine based donor–acceptor dyes (a) **D1**, and (b) **D2**, with Gaussian 09 at the B3LYP/6-31G** level of theory.

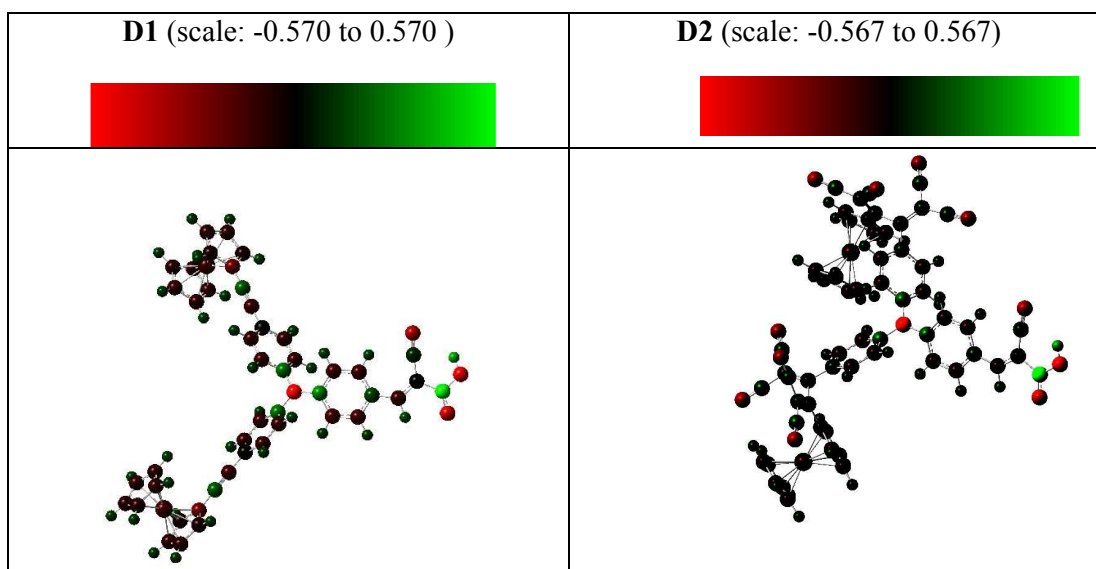


Figure 5. Spin densities for **D1**, and **D2** dyes (B3LYP/6-31G**).

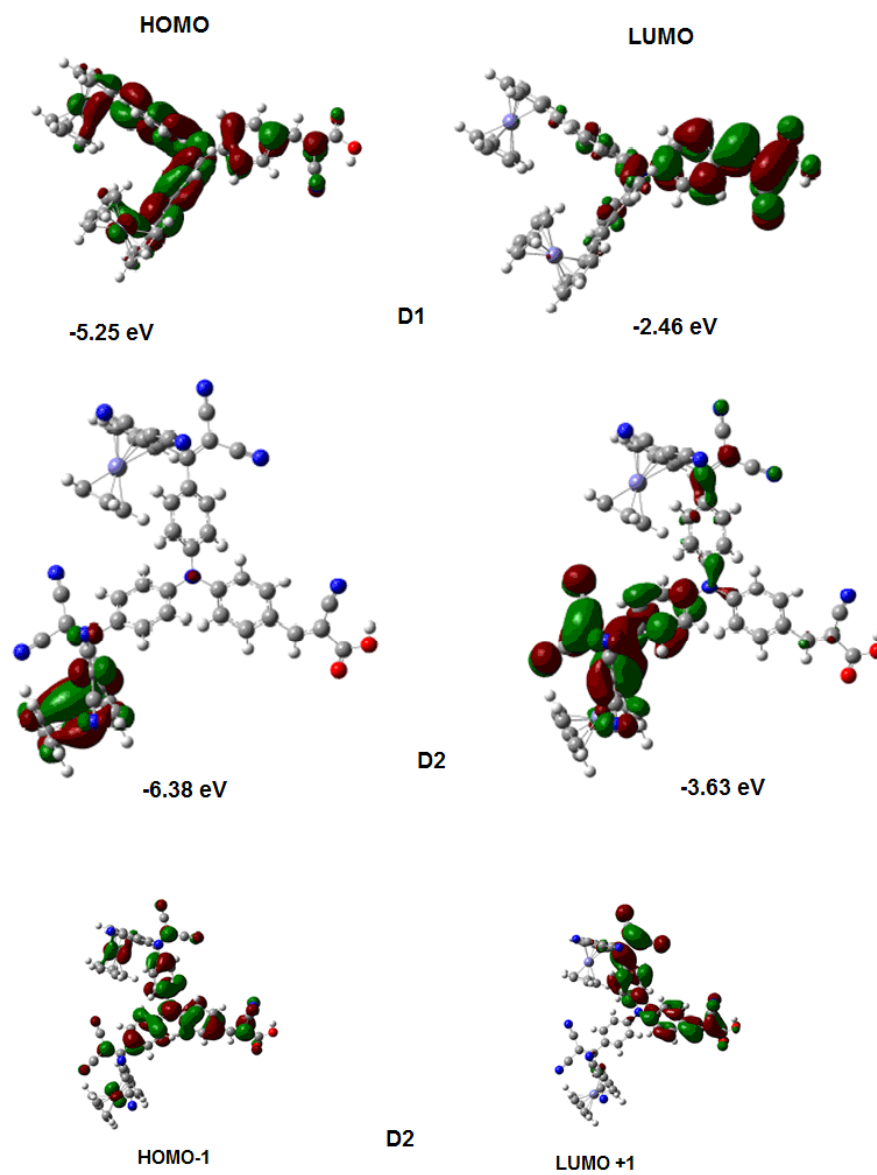


Figure 6. Frontier molecular orbitals of the ferrocenyl substituted triphenylamine donor-acceptor **D1** and **D2** dyes. HOMO -1 and LUMO +1 are also shown here.

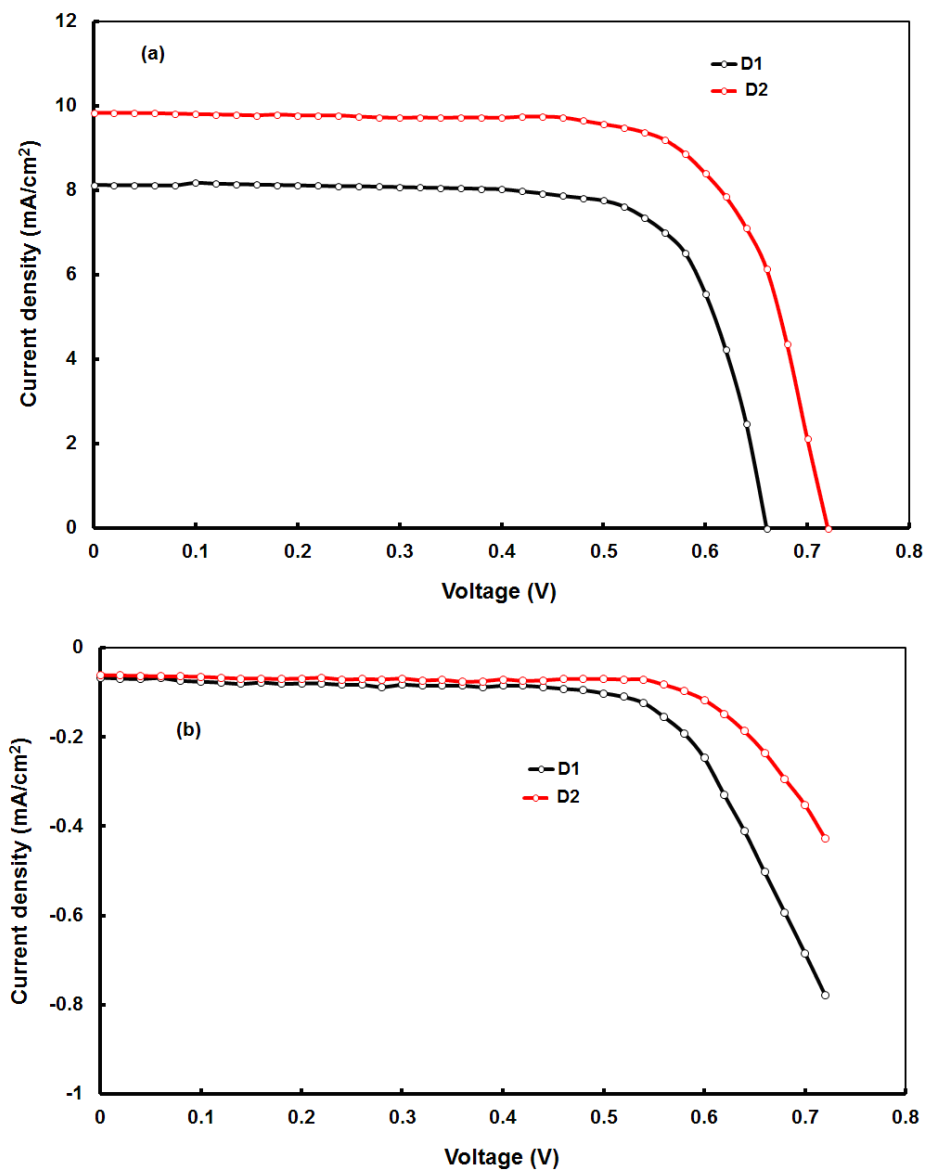


Figure 7 Current –voltage (J-V) characteristics of DSSCs sensitized with dye **D1** and **D2** (a) under illumination and (b) in dark

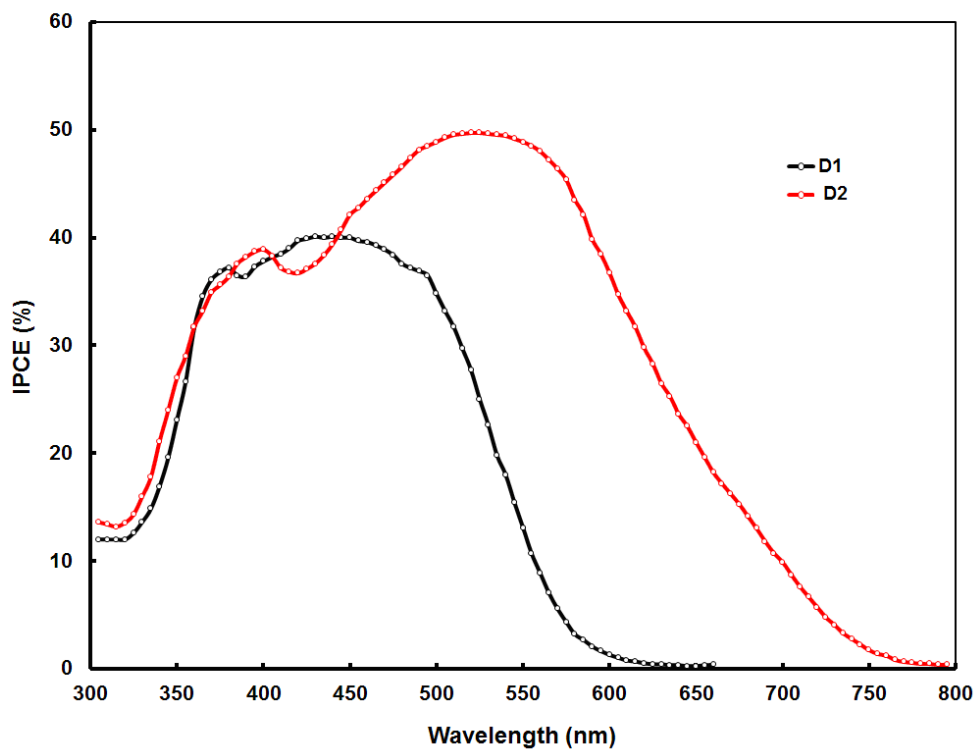


Figure 8 IPCE spectra of DSSCs sensitized with **D1** and **D2**

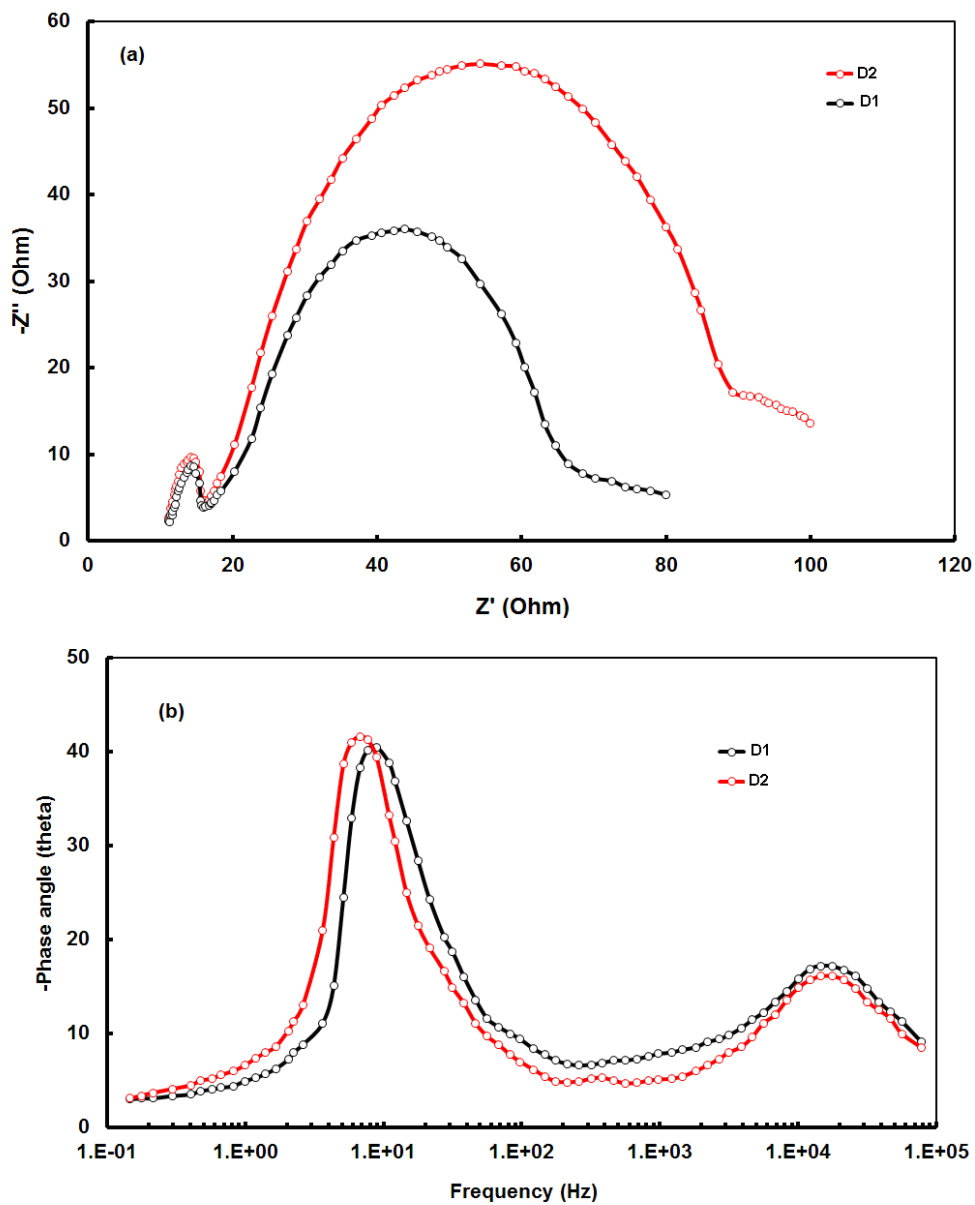


Figure 9 EIS plots (a) Nyquist plots and (b) Bode phase plots, in dark for DSSCs sensitized with dye **D1** and **D2**